Computers, Materials & Continua CMC, vol.64, no.2, pp.681-700, 2020

Image Segmentation of Brain MR Images Using Otsu's Based Hybrid WCMFO Algorithm

A. Renugambal[1, *] and K. Selva Bhuvaneswari[2]

Abstract: In this study, a novel hybrid Water Cycle Moth-Flame Optimization (WCMFO) algorithm is proposed for multilevel thresholding brain image segmentation in Magnetic Resonance (MR) image slices. WCMFO constitutes a hybrid between the two techniques, comprising the water cycle and moth-flame optimization algorithms. The optimal thresholds are obtained by maximizing the between class variance (Otsu's function) of the image. To test the performance of threshold searching process, the proposed algorithm has been evaluated on standard benchmark of ten axial T_2-weighted brain MR images for image segmentation. The experimental outcomes infer that it produces better optimal threshold values at a greater and quicker convergence rate. In contrast to other state-of-the-art methods, namely Adaptive Wind Driven Optimization (AWDO), Adaptive Bacterial Foraging (ABF) and Particle Swarm Optimization (PSO), the proposed algorithm has been found to be better at producing the best objective function, Peak Signal-to-Noise Ratio (PSNR), Standard Deviation (STD) and lower computational time values. Further, it was observed thatthe segmented image gives greater detail when the threshold level increases. Moreover, the statistical test result confirms that the best and mean values are almost zero and the average difference between best and mean value 1.86 is obtained through the 30 executions of the proposed algorithm.Thus, these images will lead to better segments of gray, white and cerebrospinal fluid that enable better clinical choices and diagnoses using a proposed algorithm.

Keywords: Hybrid WCMFO algorithm, Otsu's function, multilevel thresholding, image segmentation, brain MR image.

1 Introduction

In recent years, significant progress has been made in the field of medical imaging and computer-aided medical image analysis [Zhang, Ye, Guo et al. (2016)]. The improvements in medical imaging lead to better planning and accuracy of operations using a human machine intervention [Nilakant, Menon and Vikram (2017)]. Segmentation is important in medical imaging for extraction of features, image measurements, and display of images

[1] Department of Mathematics, University College of Engineering Kancheepuram, Kanchipuram, 631552, India.

[2] Department of Computer Science and Engineering, University College of Engineering Kancheepuram, Kanchipuram, 631552, India.

[*] Corresponding Author: A. Renugambal. Email: renutjn2016@gmail.com.

Received: 25 December 2019; Accepted: 07 April 2020.

[Yazdani, Yusof, Karimian et al. (2015)]. Numerous medical imaging technologies, such as computed tomography, magnetic resonance imaging, positron emission tomography, and ultrasound scanning are widely used in medical diagnosis [Balafar, Ramli, Saripan et al. (2010)]. Currently, the segmentation of brain magnetic resonance imaging achieves significant theoretical and application value in the analysis of medical images [Bhuvaneswari and Geetha (2014)]. Precise brain tissue segmentation can improve the reliability of brain disease diagnosis and efficacy of treatment. However, noise, gray overlap, partial volume effect, and the characteristic of different anatomic structure often affects the MR images. Since, brain images are still being studied in certain medical studies, which are labor-intensive and time consuming, by medical experts on an individual basis [Despotović, Goossens and Philips (2015)]. Therefore, anautomatic segmentation can be extremely more beneficial as it can enable the large-scale studies needed to detect subtle changes and effects of disease. Developing of fully automatic algorithms for the efficient and accurate segmentation of medical images are becoming a major medical issue [Khorram and Yazdi (2018)]. An extensive research has been carried out and several approaches have been proposed, such as clustering algorithms, threshold methods, entropy-based segmentations, etc., [Jalab and Hasan (2019); Ganesh, Naresh and Arvind (2017); Bhuvaneswari and Geetha (2016); Hosseini (2012)].

2 State-of-the-art research and proposed work

Brain image segmentation is a highly popular subject for research and numerous methods are developed. The state-of-the-art research as follows: Taherdangkoo et al. [Taherdangkoo, Bagheri, Yazdi et al. (2013)] proposed a new Ant Colony Optimization (ACO) algorithm to achieve computationally efficient results for the segmentation of medical MR images. The proposed approach utilized for four image types and showed ACO algorithm's results in segmentation and computational efficiency in comparison with other algorithms, which include Genetic Algorithm (GA) and PSO. Oliva et al. [Oliva, Hinojosa, Cuevas et al. (2017)] implemented the minimum cross entropy based thresholding criterion using a crow search algorithm. Two sets of benchmark images have been validated; the first set consists of standard images widely used in the literature for image processing while the second set refers to the MR brain images. After segmenting the brain images in various depths, qualitative analysis shows clearly defined regions which are easier to distinguish compared to other techniques such as differential evolution and harmony search algorithms. Kotte et al. [Kotte, Pullakura and Injeti (2018)] demonstrated the adaptive wind driven optimization algorithm for the optimal selection of threshold levels for brain MR image segmentation using Otsu-AWDO, Otsu-WDO, Kapur-AWDO and Kapur-WDO methods. The parametric study led to a better output of Otsu-AWDO and Kapur-AWDO approaches to all images at all threshold levels. The visibility and knowledge of the segmented images improved with increasing thresholds were observed. Manikandan et al. [Manikandan, Ramar, Iruthayarajan et al. (2014)] Proposed Real Coded Genetic Algorithm with Simulated Binary crossover (RGA with SBX) for T_2 -weighted axial brain MR images based on multilevel thresholding using Kapur entropy method. In terms of higher entropy and lower standard deviation for all images, the proposed algorithm provides better and consistent performance with the results of the existing algorithms like Nelder-Mead simplex, PSO, BF and ABF. Priya et

al. [Priya, Thangaraj, Kesavadas et al. (2013)] introduced fuzzy entropy based Modified Particle Swarm Optimization (MPSO) for MR brain image segmentation. The proposed Fuzzy entropy-based segmentation technique, optimized using a MPSO, achieves maximum entropy with proper segmentation of infected areas and a minimum time for computation, was implemented to provide successful exploration and exploitation. Maitra et al. [Maitra and Chatterjee (2008)] adopted a novel method of multilevel optimal MR brain image thresholding using bacterial foraging algorithm (BACTFOR). In the context of a number of benchmark MR brain images, the segmentation results showed that BACTFOR could overperform the PSO algorithm comprehensively. Sathya et al. [Sathya and Kayalvizhi (2011a)] applied multilevel thresholding based Adaptive Bacterial Foraging(ABF) algorithm in axial, T_2-weighted brain MRI slices to segment the white matter, gray matter and cerebrospinal fluids. The results are compared with the BF, PSO and GA algorithms in terms of solution quality, robustness and computational efficiency.The qualitative analysis showed that the 5-level threshold segments exactly than the other levels in the proposed ABF algorithm. The same authors obtained optimal thresholds by maximizing Kapur's and Otsu's thresholding functions using amended bacterial foraging algorithm [Sathya and Kayalvizhi (2011c)]. Experimental results showed that the proposed algorithm being more computationally efficient, more accurate predictions and faster converging than BF, PSO and GA. For its lowest standard deviation and highest PSNR value, the Kapur-ABF algorithm is better, whereas the Otsu-ABF algorithm gives minimal error in misclassification and converges easily. The quality of the segmentation is improved with the increased threshold level that provides the best possible threshold for the segmentation of gray matter, white matter, and cerebrospinal fluid was observed.

It is therefore evident that significant research on multi-level brain threshold MR image segmentation utilizing metaheuristic algorithms has attracted the attention of many researchers. The correct choice of the segmentation algorithm is however a difficult task in the segmentation of the brain images.In recent years, in a field called metaheuristics hybridization, the concept of efficiently combining metaheuristics has emerged. The hybrid metaheuristics main objective is to exploit the complementary characteristics of different optimization strategies [Ting, Yang, Cheng et al. (2015)]. Such hybrid algorithms have been widely used to solve problems of global optimization and examples of applications can be found in Zhang et al. [Zhang, Wang and Tong (2019); Kaveh and Ghazaan (2017); Das and Parouha (2014)]. Related to the image segmentation field, some researchers have proposed a new method of hybrid image segmentation algorithm [Bao, Jia and Lang (2019); Ewees, Elaziz and Oliva (2018)]. In the case of brain MR image segmentation, there has been less research work were found using hybridized algorithms in the literature. It is well-known that in realistic situations, majority of MR images are gray images, mostly complex with lots of information. Hence, brain MR image segmentation is still a very challenging research topic. The motivation behind this study is therefore to improve the performance of brain MR image segmentation using a newly developed hybrid algorithm.

A new hybridized Otsu-based WCMFO algorithm was therefore proposed for multi-level thresholding of brain MR image segmentation. The hybrid WCMFO algorithm is a combination of two well-known natures inspired algorithms, namely Water Cycle (WC)

and Moth-Flame Optimization (MFO) algorithms. It combines the general operators of each algorithm on a recursive basis, achieving good exploration and exploitation in WCMFO without changing their individual features.The proposed approach was compared with existing findings from AWDO [Kotte, Pullakura and Injeti (2008)], ABF [Sathya and Kayalvizhi (2011c)] and PSO [Sathya and Kayalvizhi (2011c)], which are available in the literature on ten standard benchmark T_2-weighted brain MR images based on thresholds, objective function value, PSNR and CPU time.

3 Multilevel thresholding by Otsu's function

Multilevel thresholding describes the gray levels of the image pixels of the same class within a specific range defined by multiple thresholds [Oliva, Cuevas, Pajares et al. (2013)]. This is justified by the fact that the intensity values are usually grouped in a relatively separate valley within an image histogram [Oliva, Cuevas, Pajares et al. (2013)]. Therefore, the objective is to search for the set of intensity values that would separate the image histogram into independent valleys where each valley would present an object. In the present study, the best thresholding strategies of the Otsu's method (i.e., between class variance) were taken for the proposed algorithm [Otsu (1979)].

Considering a digital image (i) having the size $H\times W$, where H is the height and W is the width. The image given can be represented by L numbers of gray levels and is considered to be {0, 1, 2, 3, ... , (L-1)}. Let N be the total number of pixels in the range which is equal to $\sum_{i=0}^{L-1} h(i)$. Here $h(i)$ refers to the number of pixels with gray level I. Then, the probability occurrence of gray level i in the image I is defined by the following equation:

$$P_i = \frac{h(i)}{N} \text{ for } (0 \le i \le (L\text{-}1)) \tag{1}$$

The thresholding based Otsu's method that divides the whole image into classes so that the variance of the different classes in maximum [Otsu (1979)] and the formalized method can be described as follows [Sathya and Kayalvizhi (2011b)]. In bi-level thresholding, the input image is divided into two classes, namely C_0 and C_1 (objects and background or vice-versa) for a threshold at a level 't'. The class C_0 contains gray levels from 0 to t-1. And, the class C_1 encloses the gray levels from t to L-1. Then, the gray level probabilities (w_0 (t) and w_1 (t)) of distributions for the gray level C_0 and C_1 of two classes as follows [Sathya and Kayalvizhi (2011b)]:

$$\mathrm{C}_0 : \frac{p_0}{w_0(t)}, \cdots \frac{p_{\mathrm{t}-1}}{w_0(t)} \text{ and}$$

$$\mathrm{C}_1 : \frac{p_1}{w_1(t)}, \cdots \frac{p_1}{w_1(t)} \tag{2}$$

where

$$w_0(t) = \sum_{i=0}^{t-1} p_i \text{ , and } L\text{=}256. \tag{3}$$

Follows that, the mean levels of μ_0 and μ_1 for classes C_0 and C_1 can be described as

$$\mu_0 = \sum_{i=0}^{t-1} \frac{ip_i}{w_0(t)} \text{ and } \mu_1 = \sum_{i=t}^{L-1} \frac{ip_i}{w_i(t)} \tag{4}$$

Then, the mean intensity (μ_T) of the whole image can be represented as follows

$$\mu_T = w_0\mu_0 + w_1\mu_1, \text{ and } w_0 + w_1 = 1 \tag{5}$$

Therefore, the below objective function of the bi-level thresholding problem the objective can be expressed as

Maximize $J(t)= \sigma_0+\sigma_1$, (6)

where,

$\sigma_0=w_0(\mu_0-\mu_T)^2$ and $\sigma_1=w_1(\mu_1-\mu_T)^2$ (7)

The bi-level thresholding is further extended to solve a multilevel thresholding problem for the various 'm' values and as follows. Let there be m number of thresholds (t_1, t_2, t_3, ..., t_m) to be selected, which divide the input or original into 'm' classes: C_0 with gray level in the range 0 to t-1, C_1 with the enclosed gray levels in the range t_1 to t_2-1,... and C_m with gray levels from t_m to L-1. The selected optimal thresholds are chosen by maximizing the following objective function and expressed as Sathya et al. [Sathya and Kayalvizhi (2011b)]:

Maximize $J(t_1,t_2,t_3,.....,t_m)= \sigma_0 + \sigma_1 + \sigma_2 + \sigma_3 + ... + \sigma_m$, (8)

where,

$$\begin{aligned} &\sigma_0 = w_0(\mu_0 - \mu_T)^2, \sigma_1 = w_1(\mu_1 - \mu_T)^2, \\ &\sigma_2 = w_2(\mu_2 - \mu_T)^2, \sigma_3 = w_3(\mu_3 - \mu_T)^2, \\ &and\, \sigma_m = w_m(\mu_m - \mu_T)^2. \end{aligned} \tag{9}$$

4 Background of WCMFO algorithm

Khalilpourazari et al. [Khalilpourazari and Khalilpourazary (2017)] proposed the hybrid water cycle moth-flame optimization (WCMFO) algorithm, which mimics the behavior of the natural flow of the water cycle and navigation of moth in nature. The proposed approach hybridizes the algorithm of WCA and MFO and named as WCMFO algorithm. The aim of developing a hybrid algorithm is to improve the performance of the optimal solution. The WCA is more capable of exploring the solution space of the problem. The streams and rivers are updating their location towards the sea, and this procedure is helping search agents to update their position on the best solution. The WCA, on the other hand, suffers from the absence of an efficient operator capable of performing exploitation [Khalilpourazari and Khalilpourazary (2017)]. While, MFO performs very well in exploitation using its spiral motion capability, but cannot efficiently explore the solution space. This is because each moth is updating their location towards their corresponding flame. Consequently, the search agents do not share the information about the best solution obtained by the MFO so far. The motivation behind to develop an

efficient WCA and MFO hybridization that can benefit from both algorithms advantages [Khalilpourazari and Khalilpourazary (2017)].

In the proposed WCMFO algorithm, the WCA is considered the basic algorithm. The WCAs first improvement is to use the moths spiral movement to update the stream and river position. The standard WCAs update procedure only takes into account the space between the stream and a river when updating a stream's position [Khalilpourazari and Khalilpourazary (2017)]. In other words, the next position of the stream would be in the space between the stream and its corresponding river. By contrast, the MFO algorithm's updating procedure allows moths to update their position around their corresponding flame anywhere. Allowing streams and rivers to update their position using the mothsspiral movement increases the hybrid WCMFO's ability to exploit significantly. The second improvement in the basic WCA enhances the raining process. In all metaheuristic algorithms, randomization plays a major role. Two processes are considered to increase randomization in the WCMFO algorithm. As in the basic WCA, the first is the raining process. The WCMFO performs raining process to create new solutions where the distance between a river or stream and the sea is less than $d_{\max}$ (i.e., distance between each river or stream and the sea). The second one uses a random walk or levy flight to allow the streams to flow randomly into the solution space. If the streams update their positions and cannot find a better solution, consider a WCA iteration, then the position of the rivers and the sea would not change until the next iteration. In the WCMFO, streams are allowed to update their position by using the following equation to increase the randomness of the algorithm [Khalilpourazari and Khalilpourazary (2017)].

$$x_{i+1} = x_i + Levy(\dim) \otimes x_i \tag{10}$$

where x_{i+1} is the next stream position, x_i is the current stream position and dim is the problem dimension or number of the decision variables [Khalilpourazari and Khalilpourazary (2017)].

$$Levy(x) = \frac{0.01 \times \sigma \times r_1}{|r_2|^{\frac{1}{\beta}}} \tag{11}$$

where r_1 and r_2 random numbers range from 0 to 1.

The parameter σ is calculated as follows based on the above formulation.

$$\sigma = \left(\frac{\Gamma(1+\beta) \times \sin\left(\frac{\pi\beta}{2}\right)}{\Gamma\left(\frac{1+\beta}{2}\right) \times \beta \times 2^{\left(\frac{\beta-1}{2}\right)}} \right)^{\frac{1}{\beta}} \tag{12}$$

5 Proposed WCMFO algorithm for multilevel thresholdingof brain MR image segmentation

As described in the previous section, the selected WCMFO algorithm for multilevel thresholding. Here, theproposed algorithm is developed to determine the position in the search space (i.e., optimal threshold values) that maximizes the Otsu's objective function. The proposed WCMFO considers a slice image of the brain MR to be processed as the test

images. This implements a multilevel thresholding process to segment white matter, gray matter, and cerebrospinal fluid of Axial, T_2-weighted brain MR image slices. This stage implements the WCMFO algorithm assisted Otsu's procedure for different threshold levels (m=2, 3, 4, 5) on the chosen test image. Later, the image quality metrics are computed for these images to discover the best threshold for segmenting the selected brain image slice. The implementation of algorithm can be summarized into the following steps:

Otsu's based hybridized WCMFO algorithm for brain MR image segmentation

Input: Brain MR image slice
Output: Optimal thresholds, segmented image, objective function, PSNR, CPU time
Step 1: *Read the MR slice brain image I and obtain the histogram, h(i).*
Step 2: *Calculate the probability distribution function using Equation (1) and obtain the histogram*
Step 3: *Initialize the WCMFO control parameters*
Step 4: *Create initial population and form sea, rivers, and streams*
Step 5: *Evaluate the fitness using Otsu's function using equation (8) and sort of selection of sea and rivers*
Step 6: *Forming the sea, river, streams and designates streams to river and the sea*
Step 7: *While i<maximum number of iterations*
i=i+1;
Step 8: *for streams*
Update the position of stream using spiral movement
Stream objective=objective function value of the new stream
if stream objective < river objective
river position= the new stream
ifstream objective < sea objective
sea position= the new stream
end if
end if
if river objective < sea objective
Sea position =River position
end if
end for
Step 9: *for rivers*
Update the position of rivers using spiral movement
river objective =objective function value of the new river
if river objective < sea objective
sea position =river position
end if
end for
Step 10: *for streams*
Update the position of the streams using Levy flightby Equation (11)
end for
for rivers and streams
calculate the distance(d) between each river or stream and the sea

if $d<d_{max}$
raining process (for both rivers and streams)
end if
end for
Linearly decrease the parameter max d
Linearly decrease the parameter a
end while

Step 11: *Keep the best solutions, rank the solutions and find the current best.*

Step 12: *Stopping criterion, if the maximum objective function value(fitness) is reached, computation is terminated. Otherwise Steps 7 to 11 are repeated.*

Step 13: *Obtain thebest thresholds for the brain MR image after computing the best objective function value.*

Step 14: *Get the Segmented brain MR image and performance metric valuesfor theselected threshold value (m).*

The overall execution involved in the proposed Otsu's based hybridized WCMFO Algorithm as shown in Fig. 1 for brain MR image segmentation.

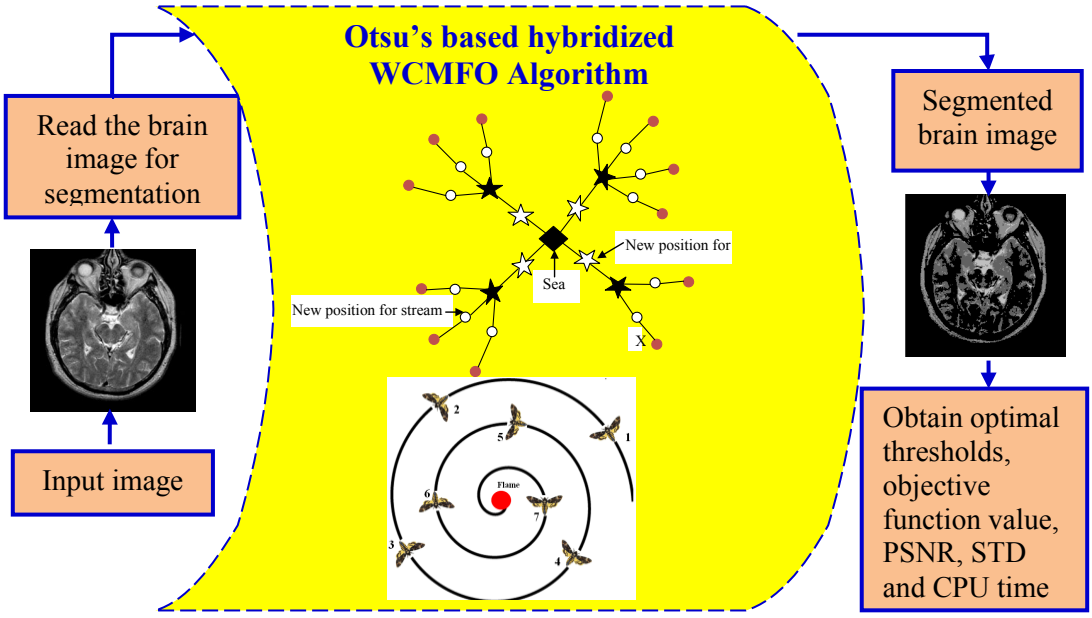

Figure 1: Execution involved in the proposed algorithm

6 Results and discussion

Consideration of the proposed WCMFO strategy is applied to the segmentation of standard 10 axial T_2-weighted brain MR images that are freely available in the Harvard medical school web-based repository of medical images. Fig. 2 illustrates a representation of the test images and each image has an 8-bit gray level of size 256×256.

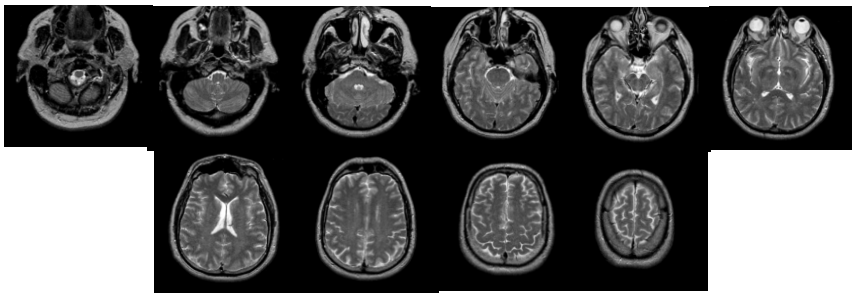

Figure 2: Standard test T_2-weighted brain MR image data set

All simulation work is performed on MATLAB 2014 with an Intel Core i3 processor with 8 GB of RAM. In proposed WCMFO, a population of the solution is formed at each dimension randomly within the limit of $[0, L-1]^m$ at the initialization stage of the algorithm. When a population is produced, a fitness value is assigned to the population's solution. The algorithm then begins to find the optimum threshold values through their selection criteria. In this case, the number of thresholds (m) represents the dimension of optimization problem. The final selected control parameters by DOE are: population size, N_{pop}=25; Number of rivers+sea, N_{sr}=4 and d_{max}=0.01. In general, the hybrid algorithm has randomized behavior. Therefore, for each image and for each m value, all experiments were repeated 30 times in order to obtain the best segmented result in terms of high fidelity evaluation. The WCMFO results (i.e., best thresholds, objective function value, and performance metric values) were compared with other meta-heuristic algorithms from the existing literature, namely AWDO, ABF and PSO. The segmented results of the proposed algorithm for T_2-weighted axial brain images with different slices were illustrated in Figs. 3-4 for the best objective values. From these Figures, it was observed that the segmented image visible high quality is better with higher levels of threshold (m=5) in assessment with m=4, m=3 and m=2 thresholds. Also, the results of the proposed algorithm are compared to other existing algorithms, as shown in Tab. 1, in terms of the obtained threshold values of the best solutions. Tab. 2 demonstrates the objective function and PSNR values. In maximization algorithm, higher the value of the objective function better is the solution. From Tab. 2, it is noted that for m=2-5 thresholds for all images, the obtained objective values of the proposed algorithm are relatively higher than existing algorithms were obtained. PSNR is a similarity between the reconstructed image and the original image [Janaki (2017)]. A higher PSNR value denotes the improved segmented image quality [Manikandan, Ramar, Iruthayarajan et al. (2014); Panda, Agrawal, Samantaray et al. (2017)]. Also, Tab. 2 lists the numerical results of PSNR for all algorithms, where the PSNR values proposed were higher than AWDO, ABF and PSO were reached. In all cases, as well as in all images, the PSNR value increases with an increase in threshold values was observed. Then, the CPU time is measure of a optimization technique that varies from different thresholds. Tab. 3 shows the CPU time and STD values of the all algorithms at different image thresholds. In consideration of CPU time, it is evidently realized that the proposed algorithm CPU time is much less than other algorithms.

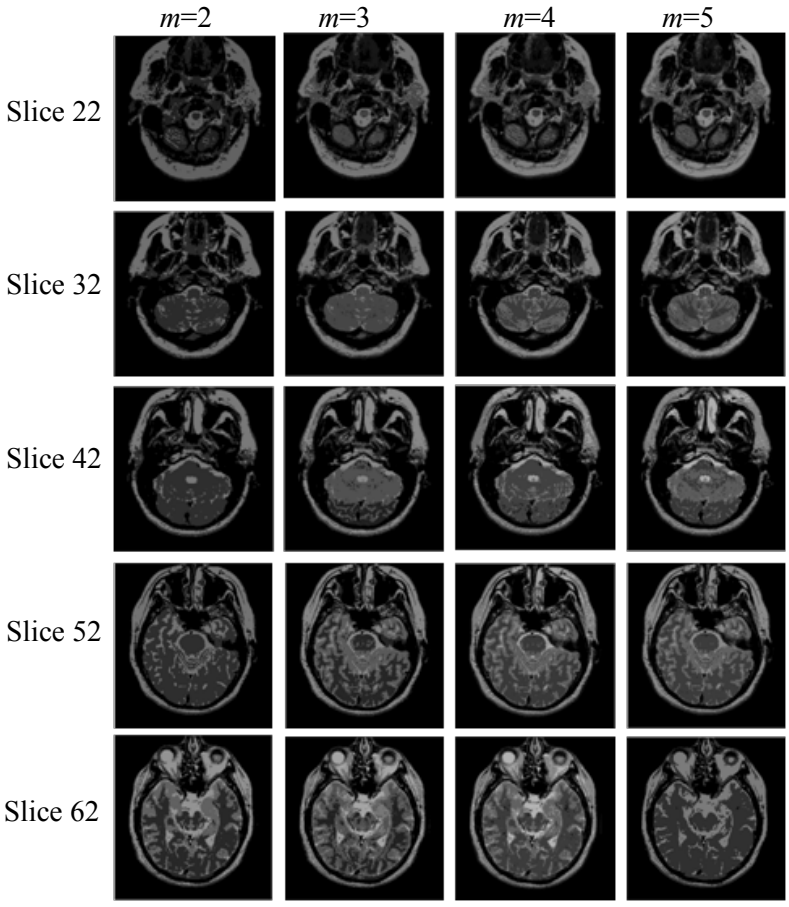

Figure 3: Results of WCMFO algorithm for the slices 22-62 images

Further, standard deviation (STD) are also computed to analyze the proposed algorithm, which measures the accuracy and stability of the objective function values. Because of the stochastic nature of metaheuristic algorithms, the solution found on each run may not be the same. Tab. 3 shows the STD values for all tested images, the WCMFO algorithm has a lower standard deviation value and therefore be concluded that, compared to other three algorithms, WCMFO performs better for multilevel thresholding. Furthermore, the algorithm statistical analysis is carried out in order to analyze the efficiency of the proposed WCMFO algorithm. Accordingly, the best, mean and worst objective function values were presented in Tab. 4 for the 30 times executions of algorithm. From the Tab. 4, it was observed that the best and mean values are almost zero and the average difference between best and mean value 1.86 is obtained through the statistical test of the proposed hybrid algorithm. Furthermore, the comparison of objective function, PSNR, CPU time and STD values are shown in Figs. 5-8, for the slice 72 image, respectively. In all the Figs, WCMFO algorithm has more sensitive to the existing algorithms for the 2-5 threshold levels. Also, the similar trend was observed for all other tested slice images.

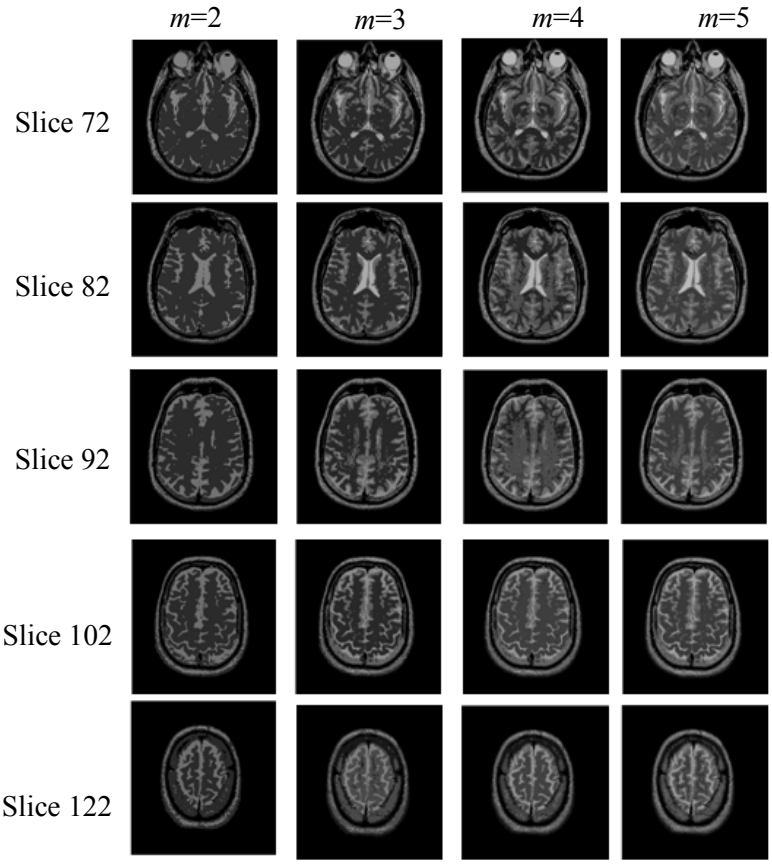

Figure 4: Results of WCMFO algorithm for the slices 72-122 images

Table 1: Best threshold values

Image	*m*	WCMFO	AWDO	ABF	PSO
Slice 22	2	33, 98	35, 99	93, 176	94, 180
	3	23, 68, 118	26, 69, 118	69, 117, 180	72, 118, 188
	4	18, 52, 90, 129	16, 44, 80, 124	50, 110, 154, 181	55, 104, 155, 200
	5	16, 44, 74, 105, 138	16, 40, 68, 101, 128	50, 86, 126, 176, 197	52, 98, 138, 187, 209
Slice 32	2	43, 113	44, 111	107, 178	108, 186
	3	24, 70, 124	23, 68, 121	70, 120, 154	73, 123, 176
	4	19, 59, 98, 136	16, 49, 89, 131	56, 96, 133, 198	60, 96, 131, 180
	5	17, 52, 85, 118, 152	14, 43, 77, 107, 144	48, 83, 119, 157, 200	49, 88, 127, 182, 203
Slice 42	2	46, 121	48, 123	112, 182	111, 186
	3	32, 81, 136	31, 84, 135	80, 122, 170	81, 125, 197
	4	21, 65, 112, 160	28, 70, 107, 154	59, 108, 144, 188	62, 107, 142, 183
	5	20, 56, 92, 129, 175	18, 58, 87, 130, 162	55, 96, 128, 158, 194	55, 118, 142, 170, 206
Slice 52	2	46, 115	43, 113	118, 188	117, 189

	3	38, 90, 134	38, 89, 132	100, 132, 171	102, 133, 174
	4	20, 60, 98, 138	19, 59, 97, 142	85, 114, 147, 184	85, 123, 172, 214
	5	19, 57, 94, 126, 166	21, 58, 87, 112, 136	60, 96, 125, 172, 197	66, 98, 130, 160, 216
Slice 62	2	48, 123	47, 123	118, 183	118, 185
	3	40, 97, 147	41, 95, 144	95, 131, 178	98, 138, 181
	4	32, 79, 119, 162	36, 84, 124, 172	80, 112, 150, 194	80, 128, 156, 193
	5	19, 60, 98, 133, 179	24, 56, 93, 132, 169	75, 106, 136, 172, 212	78, 107, 136, 172, 205
	2	46, 128	46, 127	111, 173	112, 168
Slice 72	3	41, 104, 165	44, 103, 167	105, 139, 191	106, 155, 206
	4	37, 88, 126, 183	39, 87, 128, 180	100, 128, 166, 204	101, 133, 170, 208
	5	21, 61, 95, 131, 185	18, 51, 94, 131, 177	75, 103, 132, 164, 202	76, 118, 141, 176, 216
	2	46, 125	45, 125	115, 167	114, 168
Slice 82	3	44, 105, 171	46, 99, 166	110, 141, 195	110, 166, 186
	4	35, 83, 119, 181	37, 84, 121, 179	100, 128, 162, 206	101, 134, 155, 203
	5	20, 59, 94, 128, 187	28, 57, 92, 120, 175	87, 111, 140, 185, 215	89, 120, 139, 164, 203
	2	43, 114	43, 113	100, 182	101, 180
Slice 92	3	39, 94, 135	48, 89, 129	100, 136, 194	102, 140, 173
	4	32, 76, 108, 149	27, 65, 102, 141	90, 132, 165, 191	92, 120, 148, 178
	5	19, 58, 89, 117, 155	28, 62, 88, 114, 151	90, 107, 129, 158, 196	91, 111, 138, 168, 197
	2	43, 113	43, 113	100, 158	100, 172
Slice 102	3	40, 96, 143	39, 93, 143	96, 132, 170	95, 160, 197
	4	21, 62, 101, 148	30, 61, 103, 147	90, 130, 157, 182	92, 122, 162, 199
	5	20, 58, 92, 119, 160	15, 52, 87, 113, 154	86, 108, 133, 170, 205	87, 115, 148, 183, 212
	2	42, 112	42, 111	93, 170	94, 173
Slice 112	3	25, 74, 127	27, 75, 129	76, 113, 172	78, 128, 178
	4	23, 65, 103, 147	24, 63, 103, 145	70, 108, 150, 177	70, 119, 177, 200
	5	20, 56, 86, 114, 156	22, 55, 85, 115, 154	60, 97, 140, 170, 208	62, 98, 136, 172, 194

Table 2: Objective function and PSNR values

Image	*m*	Objective function values				PSNR values			
		WCMFO	AWDO	ABF	PSO	WCMFO	AWDO	ABF	PSO
Slice 22	2	2274.62	2273.70	1808.85	1806.85	42.9934	40.9596	10.0804	9.4896
	3	2370.33	2369.60	2152.93	2134.69	48.3663	46.3073	13.2461	10.9784
	4	2409.25	2406.80	2283.98	2260.29	52.3741	49.4198	14.0166	11.4129
	5	2429.80	2426.70	2316.91	2298.89	55.8343	52.5354	16.3086	11.9047
Slice 32	2	2607.11	2606.90	1809.34	1805.70	41.4183	39.7763	9.1680	8.4334

	3	2798.48	2712.10	2550.44	2508.99	47.3643	44.6481	12.0415	9.9919
	4	2752.83	2749.60	2655.99	2638.15	51.0219	47.9352	14.7071	10.8084
	5	2773.86	2772.80	2704.02	2684.58	54.0094	51.2911	15.7517	11.3651
	2	3056.42	3044.00	2118.49	2115.50	39.8690	38.1730	9.0416	8.3074
Slice 42	3	3184.91	3143.70	2885.67	2844.73	45.6879	43.2503	12.2214	11.0724
	4	3199.43	3196.80	3117.62	3107.48	48.2982	47.1627	14.8753	11.5079
	5	3284.63	3228.60	3157.28	3127.21	52.0569	49.6585	15.6372	12.0292
	2	2884.85	2858.50	1569.43	1568.42	39.9112	37.5560	9.1512	8.2262
Slice 52	3	2946.91	2946.70	2093.42	2043.70	45.5810	43.2432	9.7967	9.2269
	4	2997.41	2996.70	2482.46	2468.60	50.0397	47.0742	11.3122	10.2423
	5	3023.63	3014.70	2932.87	2897.98	51.7949	50.2339	15.2471	14.1602
	2	3371.23	3369.40	2158.57	2156.84	38.0256	35.9739	9.1676	8.7591
Slice 62	3	3784.61	3483.30	2769.28	2716.35	42.6387	41.0956	10.4215	9.1557
	4	3536.22	3537.30	3206.05	3190.55	47.0496	44.7081	10.9746	9.8815
	5	3578.05	3574.70	3309.24	3265.68	50.1015	47.6875	13.6217	11.1006
	2	3206.15	3206.10	2082.92	2081.93	36.9944	35.1494	8.9376	8.8525
Slice 72	3	3342.15	3341.50	2263.00	2253.36	40.8987	39.4989	10.5680	9.4403
	4	3405.49	3404.30	2434.01	2377.82	45.5180	43.6053	11.0596	9.9724
	5	3441.53	3437.60	3126.95	3112.20	50.1729	45.9075	11.6371	11.3969
	2	2987.13	2938.10	1653.40	1696.23	37.6451	35.5867	9.4512	9.3187
Slice 82	3	3061.34	3056.80	1818.42	1802.72	41.4441	40.8167	9.9267	9.4671
	4	3117.07	3116.40	2099.92	2038.87	46.7559	44.9673	10.8434	9.7496
	5	3151.64	3145.50	2502.16	2432.93	51.0198	48.3557	12.1136	11.9167
	2	2653.99	2654.00	1612.49	1567.75	40.1661	38.1608	9.2776	9.2578
Slice 92	3	2744.95	2709.80	1658.76	1610.44	44.3374	45.2343	9.5888	9.3256
	4	2784.96	2749.10	1961.82	1906.44	51.2062	49.0439	10.3402	9.4954
	5	2775.54	2772.20	1980.68	1911.58	53.7791	53.0766	10.6470	10.4471
	2	2598.57	2571.60	1732.17	1719.82	41.5038	39.5085	9.3085	8.9941
Slice 102	3	2657.61	2643.00	1842.97	1820.05	45.6617	43.3470	10.1409	9.3550
	4	2682.75	2679.10	1992.94	1946.94	51.6207	48.9382	11.1441	9.9774
	5	2703.98	2702.50	2111.31	2054.13	54.6993	50.8721	11.6172	10.0065
	2	2087.61	2016.60	1843.80	1837.93	44.3057	42.0962	9.0078	8.7990
Slice 112	3	2099.17	2090.20	1896.92	1861.21	50.1450	47.6989	11.9058	8.9684
	4	2185.67	2126.30	1971.23	1954.92	53.8331	51.1259	12.6892	12.4106
	5	2141.14	2140.80	2035.33	2027.20	58.0977	55.0143	14.0649	13.7907

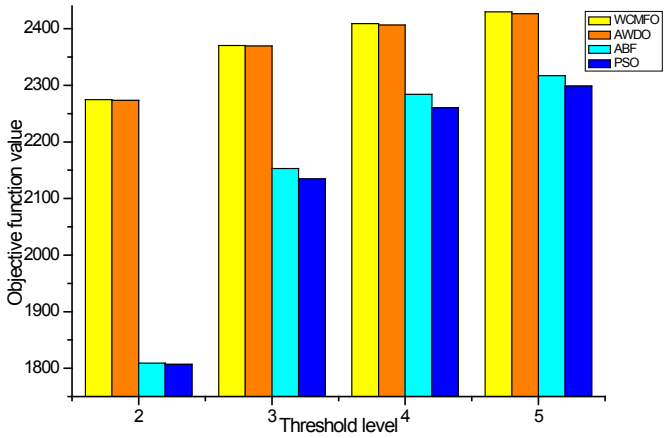

Figure 5: Comparison of objective function values for Slice 72

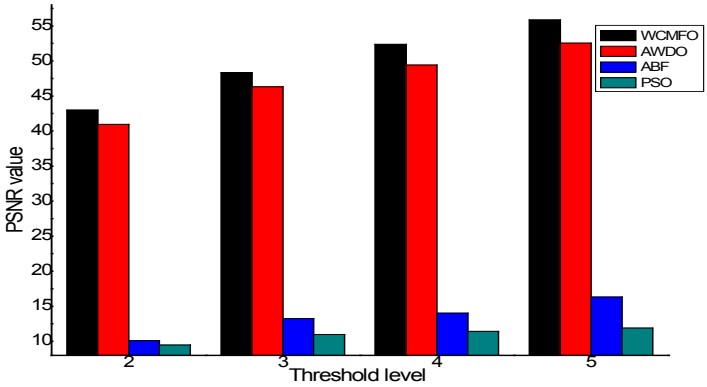

Figure 6: Comparison of PSNR values for Slice 72

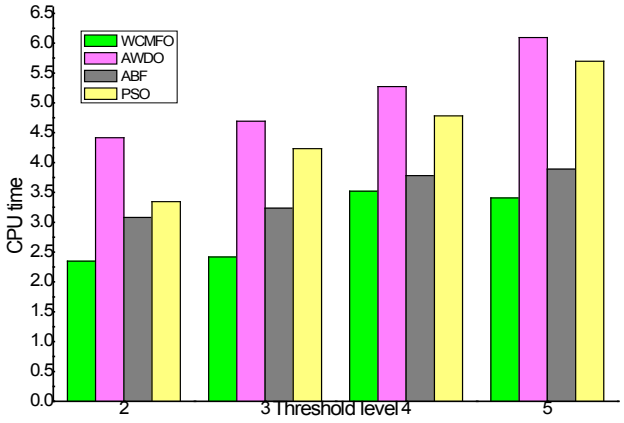

Figure 7: Comparison of CPU time for Slice 72

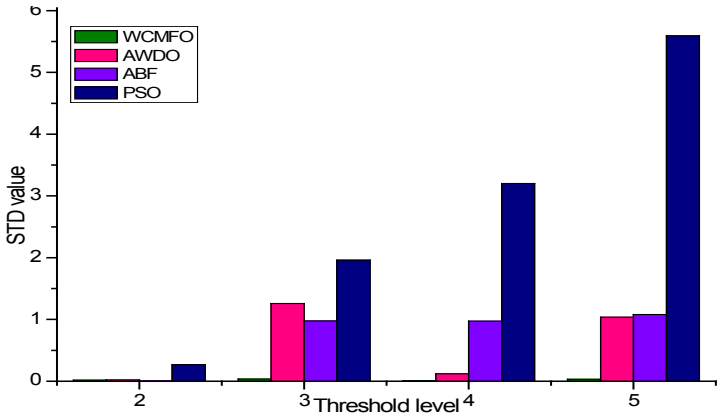

Figure 8: Comparison of STD value for Slice 72

Table 3: CPU time and STD values

Image	*m*	CPU time				STD values			
		WCMFO	AWDO	ABF	PSO	WCMFO	AWDO	ABF	PSO
Slice 22	2	2.3496	4.4142	3.0781	3.3438	0.0461	0.022	0.0021	0.2663
	3	2.4176	4.6911	3.2344	4.2344	0.0346	1.2601	0.9785	1.9609
	4	3.5210	5.2739	3.7813	4.7813	0.0075	0.1199	0.9719	3.2016
	5	3.4060	6.0944	3.8906	5.6969	0.0327	1.037	1.0811	5.5947
Slice 32	2	2.2926	3.6041	2.7969	3.1563	0.0721	1.8353	0.3119	1.5329
	3	2.4176	4.4761	3.2344	3.9063	0.0579	0.1157	0.6319	5.9255
	4	3.2074	5.2704	3.9531	4.3438	0.0415	0.4411	0.6323	6.0875
	5	4.8324	6.0995	4.6406	5.9656	0.0393	0.7957	0.5234	8.1013
Slice 42	2	2.3352	3.5875	2.7188	3.0313	0.1471	1.1012	0.2877	1.1383
	3	2.7074	4.3798	3.2031	3.9219	0.0912	0.1011	0.6169	5.2362
	4	3.2926	5.2803	3.7969	4.8594	0.0378	0.2117	0.8095	7.2116
	5	3.2074	6.8108	4.4531	5.3438	0.0407	0.1753	1.4592	9.492
Slice 52	2	2.1555	3.6388	2.7656	3.0781	0.0346	0.0388	0.1278	0.6005
	3	2.4292	4.4708	3.2969	3.9306	0.0200	0.0397	0.6771	6.1261
	4	3.1666	5.2751	3.6094	4.7656	0.0140	0.2652	1.0087	8.4673
	5	3.8960	6.0780	4.4063	5.1406	0.0376	0.3302	1.8026	9.8968
Slice 62	2	2.5304	3.5487	2.9531	3.1719	0.0021	0.2439	0.1474	1.0589
	3	2.7460	4.4317	3.1563	3.8281	0.0331	0.9368	1.0727	6.2764
	4	2.4176	5.2281	3.2344	4.1563	0.0810	0.1022	1.3146	7.0454
	5	4.1824	6.1425	4.7656	5.9063	0.0680	0.0829	1.9567	9.4338
Slice 72	2	2.3707	3.5579	2.7031	3.0781	0.0576	0.1059	0.2594	1.3353

Slice 82	3	2.6532	4.4686	3.0313	3.5156	0.0735	0.1616	0.6032	4.2687
	4	3.0852	5.5906	3.8438	4.5313	0.0641	0.2632	0.8303	6.4258
	5	3.9395	6.1703	4.5000	5.6494	0.0188	0.0325	1.1771	8.926
Slice 92	2	2.4926	3.6443	2.7969	3.1406	0.0647	0.1125	0.2731	1.553
	3	2.7052	4.4164	3.0938	3.9688	0.0223	0.0378	1.1472	4.8403
	4	3.1452	5.3712	3.5938	4.6250	0.0467	0.3407	0.5419	1.4823
	5	3.6602	6.0663	4.1563	5.2969	0.0649	0.3521	1.6522	5.0545
Slice 102	2	2.3352	3.5829	2.7188	3.0156	0.0374	0.0292	2.1028	7.0537
	3	2.4892	4.4384	2.8438	3.6406	0.0106	0.0503	1.7586	2.2252
	4	3.2102	5.2651	3.7813	4.7813	0.0509	0.367	2.3913	7.211
	5	3.1125	5.9955	4.3750	5.1052	0.0754	0.125	2.659	11.568
Slice 112	2	2.5426	3.6140	2.6719	3.0313	0.0592	0.0085	0.2828	1.2226
	3	2.7875	4.4216	3.0625	4.0313	0.0333	0.0544	1.096	5.8143
	4	3.3656	5.2372	3.4964	4.6719	0.0179	0.328	1.1994	6.5418
	5	3.0426	6.0844	4.4219	5.0625	0.0160	0.1822	1.269	7.3724
	2	2.2926	3.6196	2.7969	3.1406	0.0579	0.3982	0.292	2.4152
	3	2.4125	4.4585	2.9375	3.7969	0.0856	0.163	0.8327	4.4064
	4	3.4574	5.2713	3.8281	4.9688	0.0564	0.4441	1.6267	5.6559
	5	4.5852	6.1311	4.5938	5.6344	0.0589	0.2653	1.8955	6.8095

Table 4: Comparison of best, mean and worst objective function values for 30 Executions

Image	*m*	Best	Mean	Worst
Slice 22	2	2274.62	2273.23	2270.58
	3	2370.33	2369.36	2368.24
	4	2409.25	2408.84	2407.58
	5	2429.80	2428.44	2427.54
Slice 32	2	2607.11	2606.13	2604.87
	3	2798.48	2792.73	2790.94
	4	2752.83	2750.65	2749.33
	5	2773.86	2772.27	2771.78
Slice 42	2	3056.42	3054.96	3040.03
	3	3184.91	3181.38	3178.78
	4	3199.43	3198.61	3197.55
	5	3284.63	3283.96	3282.21
Slice 52	2	2884.85	2882.34	2881.84

	3	2946.91	2946.50	2945.28
	4	2997.41	2997.78	2996.88
	5	3023.63	3022.44	3021.78
Slice 62	2	3371.23	3369.49	3369.54
	3	3784.61	3783.84	3482.22
	4	3536.22	3533.92	3532.47
	5	3578.05	3576.43	3575.98
Slice 72	2	3206.15	3204.63	3203.45
	3	3342.15	3340.97	3339.25
	4	3405.49	3403.75	3402.87
	5	3441.53	3441.29	3440.54
Slice 82	2	2987.13	2985.98	2982.69
	3	3061.34	3060.93	3059.58
	4	3117.07	3116.27	3115.33
	5	3151.64	3150.16	3150.25
Slice 92	2	2653.99	2653.57	2652.44
	3	2744.95	2745.65	2741.98
	4	2784.96	2781.67	2779.64
	5	2775.54	2774.22	2773.86
Slice 102	2	2598.57	2591.13	2589.32
	3	2657.61	2652.89	2651.54
	4	2682.75	2682.24	2681.36
	5	2703.98	2702.96	2701.87
Slice 112	2	2087.61	2081.82	2089.63
	3	2099.17	2092.46	2088.24
	4	2185.67	2182.34	2181.21
	5	2141.14	2140.32	2139.78

7 Conclusion

In this paper, a novel hybrid WCMFO algorithm is implemented with selection best threshold values on various axial, T_2-weighted brain MR image slices for image segmentation by maximizing the Otsu's objective function. The finding were compared to those of the existing algorithms such as AWDO, ABF and PSO algorithms for analyzing the performance of the proposed algorithm. The algorithm performance was evaluated on the basis of four measures, best objective values, PSNR, STD and CPU time. Results showed that the proposed approach achieved performance for different brain MR images in the segmentation experiments. The statistical test results reveal that the average difference between best and mean value 1.86 is obtained. Conclusively, segmentation quality of the all brain MR images are better with the increase in threshold

levels that yield the best threshold in the segmentation of white and gray matters, and cerebrospinal fluid, offering the possibility of improved clinical decision-making and diagnosis.

Funding Statement: The author(s) received no specific funding for this study.

Conflicts of Interest: The authors declare that they have no conflicts of interest to report regarding the present study.

References

Balafar, M. A.; Ramli, A. R.; Saripan, M. I.; Mashohor, S. (2010): Review of brain MRI image segmentation methods. *Artificial Intelligence Review*, vol. 33, no. 3, pp. 261-274.

Bao, X.; Jia, H.; Lang, C. (2019): A novel hybrid harris hawks optimization for color image multilevel thresholding segmentation. *IEEE Access*, vol. 7, pp. 76529-76546.

Bhuvaneswari, K. S.; Geetha, P. (2014): Semantic segmentation and categorization of brain MRI images for glioma grading. *Journal of Medical Imaging and Health Informatics*, vol. 4 , no. 4, pp. 554-566.

Bhuvaneswari, K. S.; Geetha, P. (2016): Segmentation and classification of brain images using firefly and hybrid kernel-based support vector machine. *Journal of Experimental & Theoretical Artificial Intelligence*, vol. 29, no. 3, pp. 663-678.

Das, K.; Parouha, R. (2014): Optimization of engineering design problems via an efficient hybrid meta-heuristic algorithm. *IFAC Proceedings*, vol. 47, no. 1, pp. 692-699.

Despotović, I.; Goossens, B.; Philips, W. (2015): MRI segmentation of the human brain: challenges, methods, and applications. *Computational and Mathematical Methods in Medicine*, vol. 2015, pp. 1-23.

Ewees, A. A.; Elaziz, M. A.; Oliva, D. (2018): Image segmentation via multilevel thresholding using hybrid optimization algorithms. *Journal of Electronic Imaging*, vol. 27, no. 6, pp. 1-27.

Ganesh, M.; Naresh, M.; Arvind, C. (2017): MRI brain image segmentation using enhanced adaptive fuzzy K-means algorithm. *Intelligent Automation and Soft Computing*, vol. 23, no. 2, pp. 325-330.

Hosseini, H. S. (2012): Intelligent water drops algorithm for automatic multilevel thresholding of grey-level images using a modified Otsu's criterion. *International Journal of Modelling, Identification and Control*, vol. 15, no. 4, pp. 241-249.

Jalab, H.; Hasan, A. (2019): Magnetic resonance imaging segmentation techniques of brain tumors: a review. *Archives of Neuroscience*, vol. 6, pp. 1-7.

Janaki, D. (2017): Automatic brain MR image lesion segmentation using artificial bee colony optimization algorithm. *International Journal of Computer Applications*, vol. 163, no. 4, pp. 28-33.

Kaveh, A.; Ghazaan, M. I. (2017): A new hybrid meta-heuristic algorithm for optimal design of large-scale dome structures. *Engineering Optimization*, vol. 50, no. 2, pp. 235-252.

Khorram, B.; Yazdi, M. (2018): A new optimized thresholding method using ant colony algorithm for MR brain image segmentation. *Journal of Digital Imaging*, vol. 32, no. 1, pp. 162-174.

Kotte, S.; Pullakura, R.; Injeti, S. (2018): Optimal multilevel thresholding selection for brain MRI image segmentation based on adaptive wind driven optimization. *Measurement*, vol. 130, pp. 340-361.

Khalilpourazari, S.; Khalilpourazary, S. (2017): An efficient hybrid algorithm based on water cycle and moth-flame optimization algorithms for solving numerical and constrained engineering optimization problems. *Soft Computing*, vol. 23, no. 5, pp. 1699-1722.

Manikandan, S.; Ramar, K.; Iruthayarajan, M. W.; Srinivasagan, K. G. (2014): Multilevel thresholding for segmentation of medical brain images using real coded genetic algorithm. *Measurement*, vol. 47, pp. 558-568.

Maitra, M.; Chatterjee, A. (2008): A novel technique for multilevel optimal magnetic resonance brain image thresholding using bacterial foraging. *Measurement*, vol. 41, no. 10, pp. 1124-1134.

Nilakant, R.; Menon, H. P.; Vikram, K. (2017): A survey on advanced segmentation techniques for brain MRI image segmentation. *International Journal on Advanced Science, Engineering and Information Technology*, vol. 7, no. 4, pp. 1448-1456.

Oliva, D.; Hinojosa, S.; Cuevas, E.; Pajares, G.; Avalos, O. et al. (2017): Cross entropy based thresholding for magnetic resonance brain images using crow search algorithm. *Expert Systems with Applications*, vol. 79, pp. 164-180.

Oliva, D.; Cuevas, E.; Pajares, G.; Zaldivar, D.; Cisneros, M. P. et al. (2013): Multilevel thresholding segmentation based on harmony search optimization. *Journal of Applied Mathematics*, vol. 2013, pp. 1-24.

Otsu, N. (1979): A threshold selection method from gray-level histograms. *IEEE Transactions on Systems, Man, and Cybernetics*, vol. 9, no. 1, pp. 62-66.

Panda, R.; Agrawal, S.; Samantaray, L.; Abraham, A. (2017): An evolutionary gray gradient algorithm for multilevel thresholding of brain MR images using soft computing techniques. *Applied Soft Computing*, vol. 50, pp. 94-108.

Priya, R.; Thangaraj, C. K.; Kesavadas, C.; Kannan, S. (2013): Fuzzy entropy-based MR brain image segmentation using modified particle swarm optimization. *International Journal of Imaging Systems and Technology*, vol. 23, no. 4, pp. 281-288.

Sathya, P. D.; Kayalvizhi, R. (2011a): Optimal segmentation of brain MRI based on adaptive bacterial foraging algorithm. *Neurocomputing*, vol. 74, no. 14-15, pp. 2299-2313.

Sathya, P. D.; Kayalvizhi, R. (2011b): Optimal multilevel thresholding using bacterial foraging algorithm. *Expert Systems with Applications*, vol. 38, no. 12, pp. 15549-15564.

Sathya, P. D.; Kayalvizhi, R. (2011c): Amended bacterial foraging algorithm for multilevel thresholding of magnetic resonance brain images. *Measurement*, vol. 44, no. 10, pp. 1828-1848.

Taherdangkoo, M.; Bagheri, M. H.; Yazdi, M.; Andriole, K. P. (2013): An effective method for segmentation of mr brain images using the ant colony optimization algorithm. *Journal of Digital Imaging*, vol. 26, no. 6, pp. 1116-1123.

Ting, T. O.; Yang, X. S.; Cheng, S.; Huang, K. (2015): Hybrid metaheuristic algorithms: past, present, and future. *Recent Advances in Swarm Intelligence and Evolutionary Computation. Studies in Computational Intelligence*, vol. 585, pp. 71-83.

Yazdani, S.; Yusof, R.; Karimian, A.; Pashna, M.; Hematian, A. et al. (2015): Image segmentation methods and applications in MRI Brain images. *IETE Technical Review*, vol. 32, no. 6, pp. 413-427.

Zhang, J.; Wang, G.; Tong, S. (2019): Research on flight first service model and algorithms for the gate assignment problem. *Computers, Materials & Continua*, vol. 61, no. 3, pp. 1091-1104.

Zhang, Y.; Ye, S.; Guo, L.; Ding, W. (2016): Segmentation of MRI brain images with an improved harmony searching algorithm. *BioMed Research International*, vol. 2016, pp. 1-9.